Boundary-Layer Meteorol (2017) 165:311–332
DOI 10.1007/s10546-017-0268-8

RESEARCH ARTICLE

A Numerical Case Study of the Implications of Secondary Circulations to the Interpretation of Eddy-Covariance Measurements Over Small Lakes

William T. Kenny[1] · Gil Bohrer[1] · Timothy H. Morin[1,2] · Chris S. Vogel[3] · Ashley M. Matheny[1] · Ankur R. Desai[4]

Received: 22 July 2016 / Accepted: 25 May 2017 / Published online: 9 June 2017

Abstract We use a large-eddy simulation (LES) to study the airflow patterns associated with a small inland lake surrounded by a forest of height one-tenth the radius of the lake. We combine LES results with scalar dispersion simulations to model potential biases in eddy-covariance measurements due to the heterogeneity of surface fluxes and vertical advection. The lake-to-forest transition can induce a non-zero vertical velocity component, affecting the interpretation of flux measurements. Significant horizontal gradients of mean CO_2 concentration are generated by the forest carbon sink and lake carbon source, which are transported by local roughness-induced circulation. We simulate six hypothetical locations for flux towers along a downwind gradient at various heights, and calculate at each location the effects of both the average vertical advection and average turbulent-flux divergence of CO_2. We compare our model results with an analytical footprint model to find that the footprint predicted by the analytical model is inaccurate due to the complexities of advection for our test case. Similar small lakes surrounded by forests are likely affected by these phenomena as well. We recommend specialized levelling of sonic anemometers to reduce the effects of non-zero wind components. Flux towers over small water bodies should be constructed at a distance 0.5–0.67 times the diameter of the lake to provide ample separation from the areas affected by the rotor effect of the upwind forest/lake transition and the updraft at the downwind edge. Finally, we also suggest the filtering of wind directions based on the Higgins ratio.

✉ Timothy H. Morin
morin.37@osu.edu

1 Department of Civil and Environmental Engineering and Geodetic Science, The Ohio State University, 470 Hitchcock Hall, 2070 Neil Avenue, Columbus, OH 43210, USA

2 Department of Environmental Resources Engineering, State University of New York College of Environmental Science and Forestry, 402 Baker Lab, 1 Forestry Drive, Syracuse, NY 13210, USA

3 University of Michigan Biological Station, 9133 Biological Road, Pellston, MI 49769, USA

4 Department of Atmospheric and Oceanic Sciences, University of Wisconsin-Madison, 1225 W Dayton St, Madison, WI 53706, USA

Keywords Advection · Carbon flux · Footprint · Greenhouse gas · Lake · Large-eddy simulation

1 Introduction

The steady increase in emissions of greenhouse gases, such as methane and carbon dioxide, since pre-industrial times (Forster et al. 2007) necessitates direct observation and understanding of the highly variable contributions to the atmospheric greenhouse gas budget from anthropogenic and natural sources. One frequently overlooked source is inland lakes, particularly small lakes of radius within one order of magnitude of the height of the surrounding terrain. Until recently, small lakes have largely been assumed to have a negligible impact on greenhouse gas processes, primarily due to the low percentage of land area they occupy ($<3\%$) (Downing et al. 2006). As significant logistical hurdles inhibit traditional sampling and measurement techniques in these ecosystems, this assumption is difficult to verify, so that relatively little is known about how small lakes contribute to the carbon cycle globally (MacIntyre et al. 2002). As recent advances in remote sensing technology have increased the number of lakes that can be remotely detected (e.g. Feng et al. 2016), understanding the role that small lakes play in the climate system will be possible. Improvements to the observation systems of the gas exchange of lakes are critical for constraining their contributions to the global CO_2 and CH_4 budgets (Cole et al. 2007; Tranvik et al. 2009; Bastviken et al. 2011).

Net ecosystem exchange from lakes to the atmosphere is inherently difficult to measure. Common methodologies employed include floating non-steady-state chambers, or the use of chemical equilibrium with dissolved gas concentration. The drawbacks of these methods have been well documented, with the largest being the inability to account for ebullition, and the low spatial representation of point measurements, particularly in cases where the point-wise source strength may be heterogeneous (Sellers et al. 1995; Duchemin et al. 1999; Striegl et al. 2001; Vesala et al. 2006). To overcome such obstacles, the eddy-covariance technique is now being employed as an alternative methodology for the study of greenhouse gas fluxes from lakes (Vesala et al. 2006; Eugster et al. 2011; Huotari et al. 2011; Schubert et al. 2012; Mammarella et al. 2015; Podgrajsek et al. 2015).

The eddy-covariance technique has many advantages in comparison with previous methodologies, including both the ability to sample continuously over long periods of time and determine ecosystem-wide fluxes from a relatively large footprint area, in contrast to the discrete point locations observed by other methods. Even instrumentation on relatively short towers integrate fluxes over large areas ($\sim$100-m fetch per 1 m of tower height), thus significantly improving the spatial representativeness over discrete point methods. An expanded spatio-temporal coverage provides a more complete picture of the flux contribution from an entire ecosystem or portion of an ecosystem, such as a lake. However, the standard eddy-covariance technique suffers a number of limitations in regions of complex terrain. For example, under low turbulence conditions, inadequate mixing takes place, resulting in the stratification of trace gases (Reichstein et al. 2005; Barr et al. 2013), which is typically addressed through data filtering or storage calculations, thereby accounting for the build-up of gases near the surface over time (Van Gorsel et al. 2009). A second stumbling block for the eddy-covariance approach in complex terrain is the assumption that the vertical velocity is zero, which, while adequate for relatively flat landscapes, is violated in complex terrain where vertical advection is commonly encountered (Aubinet et al. 2010). Other complexities associated with complex terrain are well documented (Eugster et al. 2003; Vesala et al. 2006; Novick et al. 2014; Morin et al. 2017b). Furthermore, large horizontal roughness and

temperature heterogeneity can lead to non-random distributions of large-scale eddies (Stoll and Porté-Agel 2009; Chatziefstratiou et al. 2014; Eder et al. 2015). Similarly, it has also been shown that land-surface transitions can lead to contributions to fluxes from horizontal and vertical advection (Higgins et al. 2013) which cannot be directly measured from a single location, thus requiring multiple observation heights and horizontally-distributed observations of the concentration and wind speed. This practice is still rare due to the expense and difficulty involved in erecting an eddy-covariance tower in a lake.

An additional challenge relevant to small lakes is the lack of source homogeneity. Eddy-covariance data obtained from heterogeneous terrain are difficult to interpret due to the difference in source strengths between ecosystems (Morin et al. 2017b). Standard footprint models are commonly used to address this problem by identifying and filtering periods when the footprint lies outside of the source of interest (Knox et al. 2015). It is typically assumed that eddy-covariance observations are representative of the actual ecosystem fluxes so long as heterogeneous features, such as lake-land transitions, lie beyond the flux footprint area. However, footprint models may not accurately predict the true locations of sources in domains containing non-homogeneous topography and vegetation (Vesala et al. 2006), or as we investigate here, a land-water discontinuity. Large differences in fluxes between adjacent land-cover types can likewise introduce biases that are difficult to recognize and correct (Eugster et al. 2003; Vesala et al. 2006).

Our objective here is to test the extent of the effects of turbulence induced by surface heterogeneity on scalar fluxes from small lakes, and the bias generated by this effect relative to different configurations of hypothetical eddy-covariance tower locations and heights. We hypothesize that for small lakes, lake-scale circulations of the flow are generated by the land-lake transition and the heterogeneity of the surface roughness and heat fluxes. Such circulations distort the flux footprint away from the classical ellipse shape resulting from the introduction of non-zero average vertical velocity, which are not accounted for in standard footprint models. We also predict strong effects of proximity to the lake edge, even when the land-lake transition is downwind. Finally, we predict that the lake-scale circulations generate persistent updrafts/downdrafts, which may strongly affect flux measurements.

We use large-eddy simulation (LES) to test the potential sensitivity of eddy-covariance measurements to specific features of the airflow pattern over and at the edge of a simplified small lake. Understanding these effects is necessary for the use and interpretation of eddy-covariance observations over lakes and will provide guidance as to the type of effects that should be accounted for during experimental set-up and data processing for eddy-covariance campaigns.

2 Materials and Methods

2.1 Description of Large-Eddy Simulations

We use the Regional Atmospheric Modeling System (RAMS)-based Forest LES (RAFLES; Bohrer et al. 2008, 2009; Maurer et al. 2015) model with an explicitly-resolved canopy component. The RAFLES model resolves the flow inside and above three-dimensionally heterogeneous tree canopies after being initialized with profiles of horizontal wind speed, air temperature, and humidity, and forced by the wind speed aloft, as well as heat and water vapour fluxes at the surface. The model includes a multi-layer, three-dimensionally heterogeneous canopy, which allows the drag, volume restriction, and energy fluxes resulting from vegetation. Vegetation is prescribed as a volumetric density of leaves and resulting

aperture limitations from stems for each pixel within the canopy domain (Chatziefstratiou et al. 2014). The simulation domain (typically on the order of 1 km^3) and fine resolution (typically in the range of $2 \times 2 \times 2$ to $5 \times 5 \times 3$; $x \times y \times z$ m^3) permit the simulation of a fully-dynamic boundary layer, with a range of turbulence scales simulated within the roughness sub-layer, both inside and above forest canopies (Bohrer et al. 2009).

Our domain here consists of a 400-m diameter circular lake embedded within a horizontally-homogeneous forest of 20-m canopy height with a leaf area index (*LAI*) of 4 m^2 m^{-2} to encompass 1600×1600 m^2 in total land surface area. The albedo, vertical leaf density distribution, light attenuation coefficient, stem density, and mean stem diameters are based on the properties of the forest at the University of Michigan's Biological Station (UMBS; Gough et al. 2013; Matheny et al. 2014). The boundary conditions at the lateral domain boundaries are periodic. This periodicity can affect the flow conditions resulting from the repeated lake-forest transitions according to Dupont et al. (2011), who found transition effects extending to roughly 22 times the height of the transition. As the distance between the periodic lakes is $60H$, where H is the height of the canopy, our flow conditions have likely fully normalized within this distance.

A reflective boundary condition with Rayleigh friction for the momentum terms is applied to the topmost six grid layers to prevent amplification of boundary-induced numerical waves throughout the domain. Free-slip boundary conditions for momentum, with dynamically prescribed momentum loss due to surface friction, are applied at the bottom boundary. No-flux boundary conditions are enforced at the bottom boundary for all other terms (temperature, humidity, scalars), with a prescribed sink/source term at the surface layer, inclusive of the bottom layer and all canopy layers. A sink equal to half the instantaneous concentration of scalars is prescribed in the first two off-edge upwind vertical slabs of the model in the spanwise-vertical plain to prevent recirculation of downwind scalars back into the upwind region of the domain. The temperature, humidity and scalar concentrations are allowed to evolve throughout the simulation after being forced by their prescribed fluxes at the surface. The prescribed surface flux in each grid column is redistributed vertically within the canopy sub-layers based on the leaf-area dependent light attenuation (Bohrer et al. 2009). The vertical profile of leaf-area density was obtained from ground-based lidar observations made in the UMBS forest (Hardiman et al. 2011). We assume a light attenuation coefficient of 0.7 and the vertical redistribution of surface fluxes following the light attenuation from the canopy top for a fixed Bowen ratio with height. Fluxes above the lake are prescribed at the bottom atmospheric layer.

The initial conditions are horizontally homogeneous, including the surface-level atmospheric pressure, and vertical profiles of potential temperature, the water vapour mixing ratio, and streamwise and spanwise horizontal velocity components. Subgrid-scale turbulence kinetic energy and the vertical velocity are initialized to zero, and the initial CO_2 concentration in all grid cells is set to 15.5 μmol m^{-3} s^{-1} (385.8 ppm). We assume that the initial conditions are horizontally uniform over the entire simulation domain, including both the forest and lake, which is realistic at some height above the surface and considering that the heterogeneous turbulent local conditions develop quickly in the roughness sub-layer during the spin-up period. The horizontal wind speed is forced by adding a horizontally-uniform vertical-momentum tendency to the streamwise velocity component, equal to the mean divergence rate of the mean 30-min Reynolds-averaged streamwise velocity component from the prescribed initial wind profile due to friction. This was only applied at high elevations (above 400 m), far from the roughness sub-layer. The initial conditions and surface sensible and latent heat fluxes are based on characteristic noontime conditions for a sunny summer day

as measured by eddy-covariance towers over Douglas Lake, and at the adjacent UMBS flux tower (US-UMB) (Table 1).

The simulations have a horizontal resolution of 5×5 m^2 (dx and dy), and 2.5 m vertically (dz) near the surface. The vertical grid spacing remains at 2.5 m (dz = 0.5dx) up to 51 m above the lake surface, gradually increasing at a rate of 0.0628 m m^{-1} thereafter, until a maximum spacing of 25 m ($dz = 5dx$) at a height of 417.5 m, at which point the spacing is constant up to the top of the domain at 1542.5 m. The vertical stretching of the grid reduces the number of vertical layers to improve the simulation time, and occurs gradually to ensure the vertical dimension is between 0.5 and 5 times the horizontal dimension. The finest resolution is found in the roughness sub-layer to prevent numerical effects of turbulence anisotropy. Identical grid-stretching schemes have been applied in many previous RAFLES simulation projects without any noticeable skewness of the momentum and turbulence terms. The model timestep is 0.05 s, and the model spin-up is 3 h, with the final 30 min of the simulation used for analysis (3.5 h total). Additional formulation and details of the simulation set-up and numerical schemes are to be found in Bohrer et al. (2009) and Maurer et al. (2015).

2.2 Advection and Diffusion of Scalars (Virtual CO_2)

To facilitate the dynamic simulation of species advection-diffusion, we developed an off-line post processing that uses the formulation of the advection-diffusion (mass-conservation) equations for non-reactive scalars from the RAFLES model (Bohrer et al. 2009), where the formulation for the advection-diffusion of scalars was developed for RAMS and RAFLES models (Walko and Tremback 2001; Bohrer 2007) with subgrid-scale advection of scalars resolved using the Deardorff (1980) turbulent scheme. The fully-resolved fields of velocity, air temperature, humidity, density and pressure from the RAFLES model data are subject to post-processing rather than the original set-up of dynamic scalar advection-diffusion to facilitate experiments with different rates of scalar emissions while using the same wind fields. All equations are temporally integrated using a vectorized fourth-order Runge–Kutta approach. We perform two experiments using the output of the RAFLES simulation described in Sect. 2.1.

2.3 Simulation 1: Advection Using Realistic Fluxes

The goal of the first experiment tests to what extent advective flows of carbon are generated within the lake domain in a realistic scenario of CO_2 forest uptake and lake CO_2 emissions. This allows us to determine those areas of the lake featuring strong vertical advection that violate the eddy-covariance assumptions and, thereby, deeming them unsuitable for observational towers.

Simulation 1 features a surface boundary condition of constant homogeneous CO_2 emissions from the surface of the lake prescribed at the lowest atmospheric grid layer above the lake surface, whose strength is based on data from the lake tower. Grid cells within the forest domain remove CO_2 at a rate based on data from the forest tower at UMBS at height H. The negative carbon flux (scalar sink term) is prescribed at the top three forest layers, with half of the flux occurring in the central layer, corresponding to the layer of peak LAI, and 25% of the flux in the layers above and below. In reality, there is a positive carbon flux from the soil and uptake in the leaves. However, the precise vertical distribution of carbon sources/sinks throughout the forest canopy is poorly understood, and inclusion in the model may lead to numerical instabilities. Moreover, potentially large errors may result as the magnitudes of both the respirational source and photosynthetic sink of carbon are much larger than the net

Table 1 Meteorological data from the UMBS tower used for the simulation set-up for the initial conditions and model forcing. The air temperature, relative humidity and horizontal wind-speed profiles are from forest observations, with the mean observed values listed above near the surface are used here as initial conditions

	Sensible heat flux ($W\ m^{-2}$)	Latent heat flux ($W\ m^{-2}$)	Relative humidity (%)	Air temperature (°C)	Wind speed ($m\ s^{-1}$)	CO_2 flux ($\mu mol\ m^{-2}\ s^{-1}$)
Lake tower (≈2.5-m height)	−14.7	107.0	48.6	25.7	3.6	−20
Forest tower (46-m height)	182.8	262.4	55.6	26.4	4.0	0.00572

Values are assumed to be horizontally homogenous at initialization. The wind-speed profile above the boundary-layer top is also used for momentum forcing based on the mean noontime conditions from eddy-covariance tower data from Douglas Lake (US-UM3) and the University of Michigan Biological Station (US-UMB) for the lake and forest, respectively, on sunny days during July and August. Fluxes are prescribed at the simulation surface and vertically redistributed over several layers in the forest canopy. Fluxes take the micrometeorological sign convention, which is positive upwards into the atmosphere and negative downwards into the ecosystem

flux measured at the above-canopy tower. All driving data are derived from average values for a summer day at noontime as measured by the Douglas Lake eddy-covariance station (US-UM3) (Table 1) (Morin et al. 2017a) and from the UMBS forest station (US-UMB; Gough et al. 2009, 2016).

2.3.1 Flux Calculations

Large-eddy simulations and post-processed model results are used to calculate the turbulent and advective fluxes at each point throughout the domain as the temporal average of the product between the vertical velocity perturbation and concentration perturbation at each point within the domain. Perturbations are calculated using Reynolds averaging over the entire horizontal extent of each vertical grid layer every LES timestep [(for further details, see the formulation and definition of the model-domain flux calculation in Maurer et al. (2015)]. This approach can only be used in the LES model where the full two-dimensional field is known. Subgrid-scale components are modelled by linearly interpolating the concentration across grid cells. Flux towers, where only a point measurement is available, must diverge from the Reynolds-averaging formulation and substitute time for space using the perturbations from the 30-min averaged time series rather than the spatial perturbation from the Reynolds-averaged spatial fields. The vertical advective flux is calculated by multiplying the 30-min mean vertical velocity by the 30-min mean local vertical gradient of CO_2 concentration across each grid point.

2.4 Simulation 2: Virtual Tracer Test for Explicit Footprint Modelling

A heterogeneous terrain with multiple land-cover types may also lead to measurement bias due to horizontal concentration gradients and advection from neighbouring land-cover types. For example, the high uptake of CO_2 by a forest results in a low CO_2 concentration above the forest. The horizontal velocity component advects CO_2 from the lake towards the forest below the tower height, and thus, a lake-based eddy-covariance tower may not account for any advected fraction of CO_2 flux that originated from the lake. We address this potentially confounding influence through the use of a tracer-release experiment, which allows us to explicitly determine the footprint of carbon flux observed by a virtual tower over the lake, and examine how the tower location influences both, (1) the ratio of lake and forest contributions to flux observations, and (2) the vertical flux divergence as a function of height over the lake domain. We use the tracer experiment combined with a traditional analytical flux footprint model to determine the extent to which the analytical footprint adequately estimates the true origin of fluxes.

To simplify the interpretation of the results, simulation 2 is conducted with a fixed, horizontally homogeneous scalar flux, which eliminates the confounding effects of flux source/sink heterogeneity, and allows us to isolate effects due to advection and turbulence patterns generated by roughness and heat-flux heterogeneities. We use nominally different virtual scalars with the same properties for fluxes from each sub-region in the simulation domain to trace the source-area composition of the explicitly-resolved footprint at each virtual tower location in the simulation domain.

The domain for simulation 2 is divided into the five zones shown in Fig. 1d, which include three concentric circles in the lake (Z_{rim}, near shore; Z_{int}, intermediate; and Z_{cent}, lake centre) and two quadrants of forest ($Z_{f,up} - Z_{f,dn}$, for the upwind and downwind sections of the forested sub-domain, respectively). Each zone releases a unique tracer from each grid cell at the surface layer within its domain. All scalars are emitted at an arbitrary source

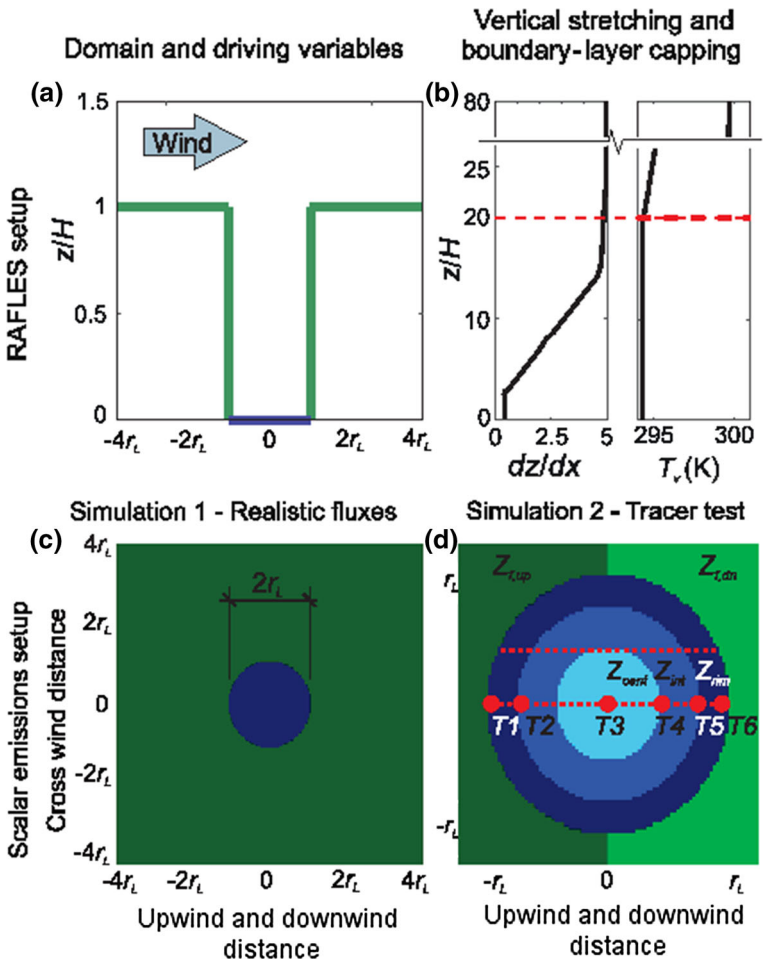

Fig. 1 Domain set-up for the RAFLES simulations: **a** vertical cross-section. Only a small portion of the vertical domain is shown to better illustrate the set-up near the lake and canopy surfaces. The *green lines* show the forest of height $H = 20$ m surrounding the inland lake (*blue line*). The direction of streamwise velocity forcing is illustrated with an arrow; **b** the grid-cell vertical spacing and initial profile of virtual temperature. The boundary layer extends to $20H$, where the virtual temperature inverts. The dz ratio gradually increases from 0.5 dx to 25dx; **c** set-up of CO_2 flux forcing in it simulation 1: Bird's-eye view of the lake. Realistic fluxes are prescribed to the lake and forest to examine flux signatures and advection patterns; **d** domain configuration for *simulation 2*. Different virtual scalars are released from each zone of the domain (Z_{cent} Z_{int} *and* Z_{rim} for the centre, intermediate, and rim sections of the lake and $Z_{f,up}$ and $Z_{f,dn}$ for the upwind and downwind sections of the forest) to track the dispersion from different domain locations. Virtual tower locations, labelled and referred hereafter as $T1$ through $T6$, ascending from west (upwind) to east (downwind) are chosen for analysis. The *dashed red lines* indicate the two transects (centre and off-centre) where flux divergence patterns are analyzed

strength of 1 scalar m^{-3} timestep^{-1}. In the lake portions of the domain, the scalar is released at the lowest grid cell to simulate the surface flux from the lake. In the forest, the scalar is released from three layers representing the upper layers of the canopy with the same vertical distribution as simulation 1. In this simulation, scalars leaving one side of the boundary are not reinserted, so that the fate of scalars from each portion of the domain can be tracked

to determine the implications of the turbulence induced by surface heterogeneity on scalar transport and fluxes downwind of the sources.

2.4.1 Footprint Model

Simulation 2 was designed to evaluate the validity of a commonly-used footprint model for situations of heterogeneous terrain, such as the lake simulated here. We use a footprint model forced with the same meteorological conditions as the RAFLES model to trace the probability that the fluxes observed at a virtual flux tower originated from any specific point in the domain, and compare with the flux of scalars predicted by simulation 2 at each virtual tower location. The footprint model is a multi-patch extension of the two-dimensional model reported by Detto et al. (2006), which is based on the one-dimensional model reported by Hsieh et al. (2000), and expanded, described, and used in Morin et al. (2014). The footprint model takes wind speed, wind direction, roughness length, displacement height, boundary-layer stability, and turbulence observations into account to trace the probability that a parcel of air measured at a particular location representing the top of an observational tower originated from any particular point in the simulated lake domain. We calculate the footprint from the 30-min averages of the same RAFLES model data and meteorological data used to drive the advection-diffusion simulations at six virtual tower locations (see Sect. 2.5 and Fig. 1). The model generated an ellipse-shaped footprint area for each 30-min average, defined such that there is a 90% probability that the observed flux originated from that area. The infinite tail of the probability distribution (accounting for the remaining 10%) is truncated, and the partial contribution of each patch type within the footprint area is integrated to determine the final footprint percentage of each land-cover type.

2.4.2 Virtual Tower Locations

In simulation 2, we perform domain-wide and lake-wide analyses to study the effects of different phenomena that may bias flux observations. To quantitatively assess the impact of the domain structure on virtual eddy-covariance measurements, we select a number of locations within the simulation domain to be virtual towers (Fig. 1) based on an evenly spaced transect along the lake in the primary wind direction. At each location, we consider the simulated flux of each scalar at heights of 5, 20, and 40 m corresponding to $0.25H$, H, and $2H$, respectively. We compare the composition of these fluxes to the predicted contribution of each section and to the observed total scalar flux as evaluated by the traditional footprint model (described in Sect. 2.4). In this simulation, $0.25H$ (5 m) is located in the second vertical grid layer and provides a conservative limit for the adequacy of tower locations. An analysis of shorter virtual towers could not be performed at the lowest grid layer since the location of the prescribed scalar flux is found within the same layer. While shorter towers are frequently employed to constrain the extent of a tower's footprint in practice, fluctuations in water level often limit the minimum height above the water surface at which sensors and equipment may be deployed without risking flood and splash damage. In general, heights of 2–5 m is a realistic range for real-world lake towers (Anderson et al. 1999; Vesala et al. 2006; Eugster et al. 2011; Morin et al. 2017b).

We analyze the vertical flux divergence to assess advection as described in Higgins et al. (2013) and Novick et al. (2014), which is an indicator of the horizontal advection to and from a parcel of air causing an imbalance in fluxes between two nearby vertical points. Eddy-covariance towers often quantify advection through the change of storage under the

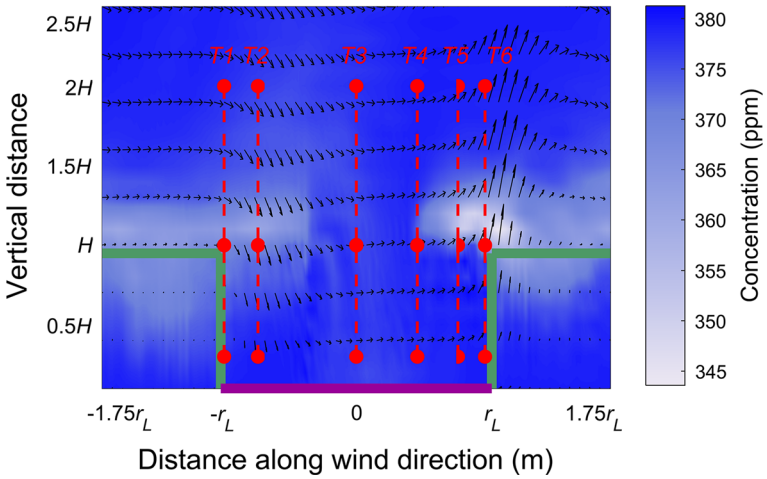

Fig. 2 *Simulation 1*: vertical cross-section of the domain through the centre of the lake parallel to the mean horizontal wind direction. The mean wind speed and CO_2 concentrations over the 30-min simulation are shown. The image is stretched in the vertical direction and the vertical velocity component is exaggerated relative to the horizontal to illustrate the non-zero mean vertical velocity component, as well as rotor and ejection effects on scalar concentrations. The *purple bold line* at the *bottom* of the domain represents the lake surface, and *bold green lines* represent the forest surrounding lake. *Vertical red dotted lines* indicate the simulated tower locations with the *large red dots* showing the virtual tower heights

sensor location. We account for storage for the 30-min flux calculations to simulate what could feasibly be accounted for using traditional eddy-covariance processing techniques. All Reynolds-averaged fluxes accounted for the storage flux, where

$$S = \sum_{i=1}^{z_0} \frac{\mathrm{d}C}{\mathrm{d}t} \mathrm{d}z \tag{1}$$

where z_0 is the 'measurement' height, C is the CO_2 concentration, and S is the storage under the tower. The flux divergence is calculated from the adjusted flux values by taking the difference in fluxes between two adjacent horizontal planes. The uncertainty of flux divergence is determined by taking the standard deviation of the flux divergence in the central six grid cells in the y-direction at each point along the wind direction.

3 Results and Discussion

3.1 Simulation 1: Flux Analysis and Vertical Advection

From the realistic case (simulation 1), we calculate time-averaged wind-speed patterns throughout the domain, CO_2 concentrations, and fluxes for the 30-min simulation, representing typical summer noontime conditions (Fig. 2).

Notably, over much of the lake domain above $0.5H$, and especially near the transitions from forest to lake, the 30-min mean vertical velocity component is non-zero, which violates the assumption that is central to the interpretation of eddy-covariance measurements (Novick et al. 2014). A typical backward-facing step-induced rotor effect (Cassiani et al. 2008; Detto et al. 2008; Chatziefstratiou et al. 2014) can be seen with wind gusts over the upwind edge

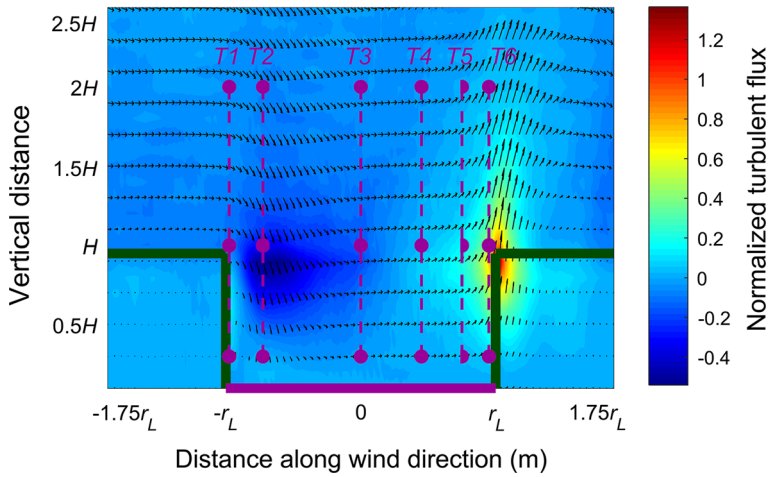

Fig. 3 *Simulation 1*: total flux at each point over a vertical cross-sectional domain through the centre of the lake, parallel to the mean horizontal wind direction. Fluxes have been normalized with respect to the forest-flux strength. *Dark green* and *purple bold lines* represent the forest and lake, respectively, as in Fig. 2, and the image is similarly stretched in the vertical direction. The *vertical dotted purple lines* indicate virtual-tower locations with the *large purple dots* indicating the simulated heights. Data are normalized to the lake fluxes

of the forest and down into the open air above the lake, cycling upwind under the forest canopy, and finally ejecting upwards above the forest (Fig. 2). A forward-facing step-induced circulation can be observed at the downwind edge of the forest, with a persistent uplift zone slightly downwind of the forest edge (Dupont and Brunet 2008a, b; Belcher et al. 2012; Chatziefstratiou et al. 2014). Depending on the measurement elevation and location with respect to the lake edge, these rotors generate horizontal advection of CO_2 either to or from the lake, and non-negligible vertical advection of CO_2, which biases flux measurements that both neglect horizontal advection and assume the mean vertical wind speed is zero.

Figures 3 and 4 present the total and the vertical advective component of CO_2 flux, respectively. The strong positive and negative fluxes of CO_2 observed near the lake-forest transitions at all heights, from zero to $2H$, are driven by local jets that evolve due to the forward- and backward-facing step-type flow obstruction posed by the forest-lake transition. The upwards jet at the downwind and rotor flow at the upwind sides of the lake are typical of sub-mesoscale flow at a characteristic length scale of a few times the canopy height (Eder et al. 2015). A complex interpretation of these phenomena would be required to account for their effects on eddy-covariance measurements, since an analytical correction for such effects over a broad range of canopy heights and surface-heat-flux gradients is currently lacking. The presence of persistent updrafts and downdrafts, which are particularly problematic for the standard three-dimensional coordinate rotation used to correct for an imperfectly levelled sonic anemometer, result in the erroneous rotation of the coordinate system to counter the persistent downdraft over the lake, and particularly, the updrafts and downdrafts near the forest-lake transition. While several approaches for coordinate rotation in the processing of eddy-covariance data exist, a persistent non-zero vertical velocity leads to a bias regardless of the approach used. A three-dimensional rotation based on the 30-min averaged flow forcing the vertical and crosswind components to zero (Lee et al. 2004; Su et al. 2008) lead to the largest error.

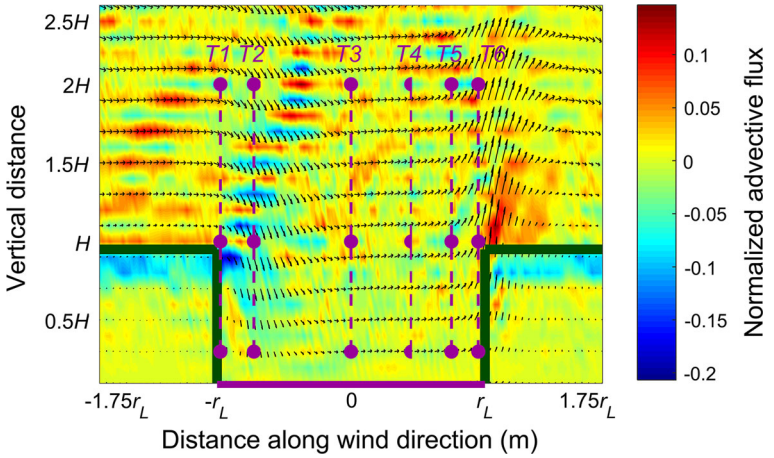

Fig. 4 *Simulation 1*: average vertical advective component of the vertical fluxes over the same cross-sectional domain. Data are normalized to the forest-flux strength

A rotation more commonly applied over non-flat terrain based on the planar-fit to long-term three-dimensional wind directions as typically applied over non-flat terrain (Finnigan et al. 2003), also produces a bias. In this case, the correction attributes a non-zero vertical velocity component to the complex topography, and thereby negates the vertical components of any jet-like flow structures. Hence, this approach assumes sloping topography at the upwind and downwind forest-lake transition zones. Note that our simulations may diverge from reality with respect to the simplified spatial scheme used for the lake (circular) and forest fluxes (horizontally homogeneous canopy sink at three top forest layers without direct soil source at the forest floor). The presence of a large soil-respiration flux below the forest canopy and a strong photosynthetic uptake by the leaves may lead to strong lateral advection in opposing directions (towards the lake near the ground, and from the lake at higher elevations) in cases where sub-canopy thermographic flows develop when the canopy air is decoupled from the flow above the canopy (Froelich and Schmid 2006). This does not typically occur during the daytime with moderate wind speeds, i.e. in conditions typical for the growing season used here. However, under stable conditions at night and in winter, decoupled sub-canopy flows may develop and further complicate the flux-source mixing between the lake and forest. It is important to note that such conditions would primarily be present at times when photosynthesis is very low or absent (night, winter) and, thus, when both the lake and forest are carbon sources (Froelich et al. 2005). We did not simulate such conditions in the present study. In real-world eddy-covariance observations, measurements during stable conditions, and at times when surface flows are decoupled from higher elevations, are typically discarded by the friction-velocity threshold filter for turbulence mixing used for quality control in standard eddy-covariance data processing (Vesala et al. 2012).

3.2 Simulation 2: Footprint Analysis and Flux Divergence of Scalars

We compare the relative-flux contribution from each section in simulation 2 to the footprint model predictions. For a tower located at the centre of the lake ($T3$) with a measurement height equivalent to the canopy top (20 m) (Fig. 6), the footprint model predicts that 43% of the observed flux originates from the lake and 47% from the upwind forest area, not including

an additional ≈10% from the far tail of the continuous infinite footprint distribution that falls outside the simulation domain. Our LES results indicate a much stronger contribution (93.9%) of the upwind forest (i.e. scalars originating from $Z_{f,up}$) to the flux observations at the centre of the lake, which results from the secondary circulation patterns driven by the forest edge (Fig. 5).

We show the contribution of every flux source location for each virtual-tower location (see Fig. 1) at heights of 5 m ($0.25H$—a typical height for lake flux towers), 20 m (H—where we expect heterogeneity effects to be maximum), and 40 m ($2H$). The typical height recommended for the measurement of forest fluxes is 1.5–2H, depending on the displacement height of the forest (Aubinet et al. 2012). As expected, the predictions of the footprint model for tower locations near the upwind forest-lake transition (locations $T1$ and $T2$) are the least representative of the 'true' flux footprint generated by simulation 2 (Fig. 6).

The implications of the rotor and vertical advection flows are evident through the fate of scalars originating from both the lake and forest (Fig. 2), which, from the upwind portion of the lake, are likely to be cycled downwards towards the lake surface and may skew measurements further downwind. Moreover, the influx of scalars from the forest reveals the potential for upwind sources to skew measurements over the lake as they are swept downwards into the air above the lake.

Agreement between the footprint model and LES-based explicit footprint calculation is strongest in the downwind portion of the lake. In all downwind-of-centre cases (locations $T4 - T6$), the sign of the zonal contributions is consistent between the footprint model and the LES model. However, the magnitudes of the relative contributions from the forest and the lake, as well as the different zones within the lake, are rarely similar. The apparent optimal tower location of the subset analyzed is location $T4$, which is located 300 m downwind from the lake edge, at three-quarters of the lake's diameter and of a height of 1.5H. The 5-m height ($0.25H$) at this tower location represents a ratio of 0.0167 between measurement height z_1, and the distance to the upwind transition D_T, which meets the criterion suggested by Higgins et al. (2013) of $(z_1/D_T) < 0.02$ for minimizing the effects of advection. As such, it is expected that a low measurement height at a distance far enough from the upwind transition could increase the representativeness of eddy-covariance results for a lake of this size, similar to Vesala et al. (2006). However, the presence of additional flux sources/sinks in the ecosystem surrounding the lake complicates the interpretation of the measurements due to the downward vertical advection of scalars from the overlying air and the complex upwind and downwind lateral advection pathways away from the lake edges.

While at $z_1/D_T < 0.02$ the magnitude of these contributions to the overall flux is relatively small, their absolute effect depends on the relative magnitude of scalar fluxes in the lake and surrounding ecosystem. As we nominally prescribe a uniform flux strength at all sources here, the contribution of non-lake carbon to the flux observed at location $T4$ at 5 m above the lake surface is roughly 30% (Fig. 6). However, observations show that noontime carbon uptake rates from the surrounding forest at our site in Michigan are on the order of 10 μmol m^{-2} s^{-1}, whereas the lake is a comparatively small source on the order of 1 μmol m^{-2} s^{-1}, further skewing the measurements at this location towards the contribution of the forest. The temporal variability of the source/sink strength difference leads to increased uncertainty.

3.2.1 Vertical Flux Divergence

We use the vertical flux divergence of the scalars to analyze the implications of the domain structure on fluxes. If a flux remains relatively constant across all heights at a potential tower location, then the contribution of advection to the mass budget between two heights is

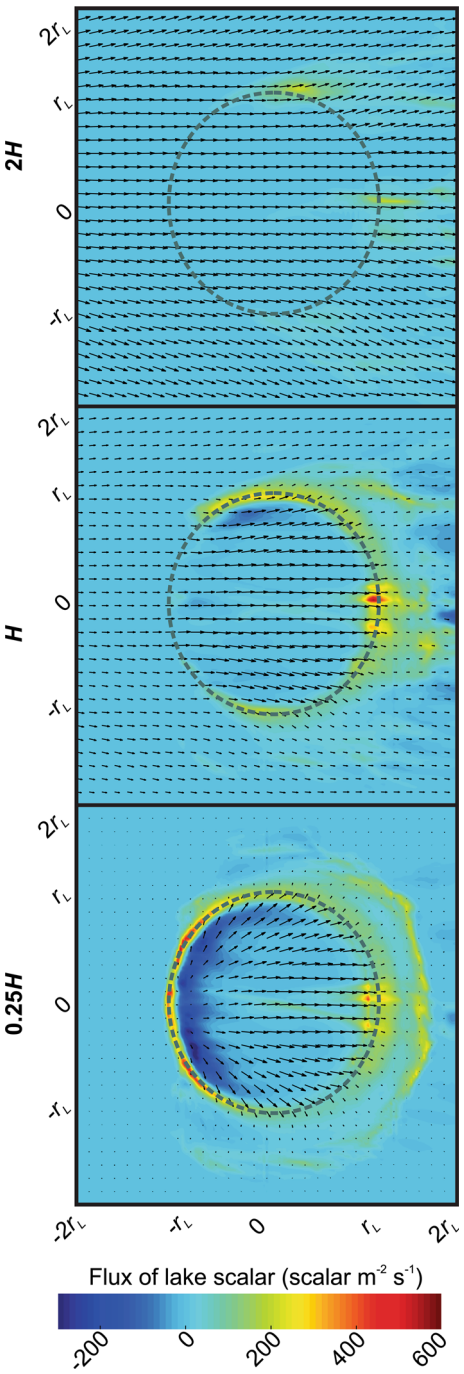

Fig. 5 *Simulation 2*: top view of 30-min averaged scalar flux originating from the lake. Positive fluxes are towards the atmosphere, while negative are towards the ground. *Arrows* indicate the mean horizontal wind speed and direction. The lake (radius r_L) area is shown by the *dashed circle* in each figure. Here, the three different heights considered in our discussion are shown: 5 m ($0.25H$, *bottom*), 20 m (H, *middle*), 40 m ($2H$, *top*)

minimized (Novick et al. 2014), thus indicating that the measurements at those two heights are an accurate reflection of vertical contributions to the turbulence flux. Similar to the previous analysis, upwind tower locations (e.g. location $T2$) show a strong height-dependent vertical

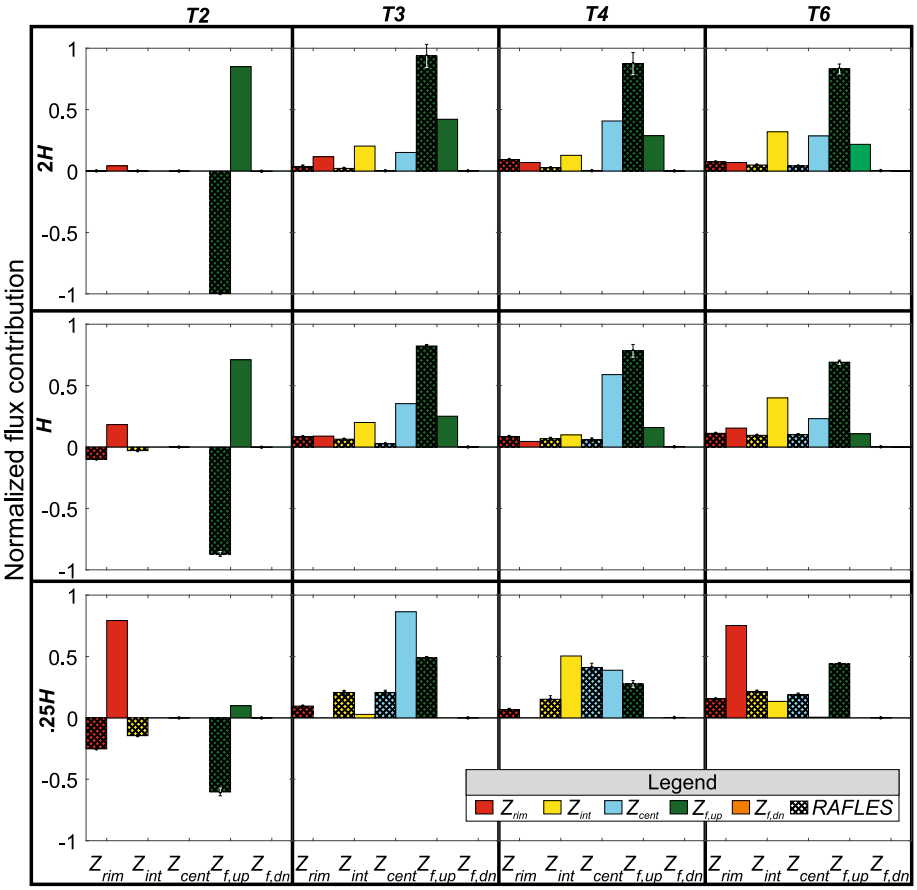

Fig. 6 *Simulation 2*: relative flux contribution from different zones of the domain as predicted by the footprint model (*right bar* of each colour, no hatching) and LES (*left hatched bar* of each colour) at various locations and heights

flux divergence, indicating significant advective contributions to observed fluxes at those locations (as shown for location $T2$ in Fig. 7).

Locations further downwind from the lake-forest edge show smaller magnitudes of flux divergence at lower heights (Fig. 7, locations $T4$ and $T5$). The simulated measurements from the region between $0.5r_L$ and $0.75r_L$ downwind of the lake centre at both high ($1.5-2.5H$) and low heights (closer to the lake surface, $0.25-1H$) show relatively low levels of vertical flux divergence, indicating that measurements within this zone are not strongly biased by advection. However, locations near the upwind and downwind edges of the lake at both low and high elevations will be biased by advection. The flux divergence is consistently highest at the canopy height.

The sum of the vertical flux divergence for every location in the lake is computed by considering scalars that originated from the lake and the forest separately, and as a total of the two (Fig. 8). We also consider "low tower" and "high tower" scenarios, whereby the summed vertical flux divergence from 3 m to 10 m represents the sum of the flux divergence in the vertical space surrounding the $0.25H$ tower height, and the summed vertical flux

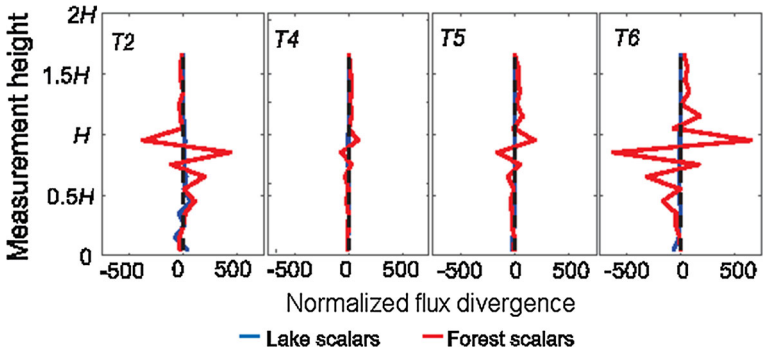

Fig. 7 *Simulation 2*: profiles of vertical flux divergence for scalars that originated from the lake surface and from the forest for location $T2$ (0.75 of the lake radius upwind of lake centre), location $T4$ (0.5 of lake radius downwind of centre), location $T5$ (0.75 of lake radius downwind of centre) and location $T6$ (downwind lake edge). Fluxes have been normalized by the effective planar emissions set in simulation 2

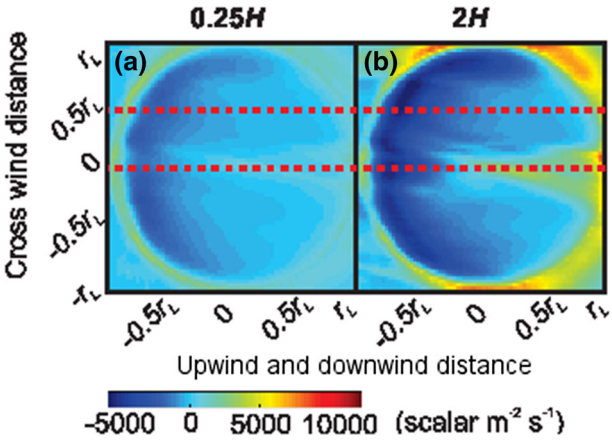

Fig. 8 *Simulation 2*: top views of the lake area. The *colour* shows the sum of the flux divergence ranging from 3 to 10 m—representing the height of a low tower of $0.25H$ (*left column*) and from 5 to 40 m—representing the high-tower height of $2H$ (*right column*) at each $x - y$ location in the domain. *Red dotted lines* show the horizontal transects analyzed using the summation of the flux-divergence approach (Fig. 9)

divergence from 5 m to 40 m represents the sum of flux divergence up to the $2H$ tower height, for the low- and high-tower scenarios, respectively. The overall pattern of summed fluxes is similar over the lake in each case, with regions of positive, negative, and close-to-zero total flux divergence occurring in essentially the same places in each of the scalar and height combinations. These results indicate that the geometry of the domain generates the same zones of low flux divergence regardless of the origin of the scalar or the height of measurement, suggesting that an optimal tower location is possible for measurements at various heights. Our findings demonstrate that eddy-covariance stations should be placed off-centre in the lake to maximize the distance between the forest-lake transition in the primary wind direction and the tower. However, the transition in the opposite direction must also be considered, as the influence of the boundary is likewise apparent for towers placed too close to the forest.

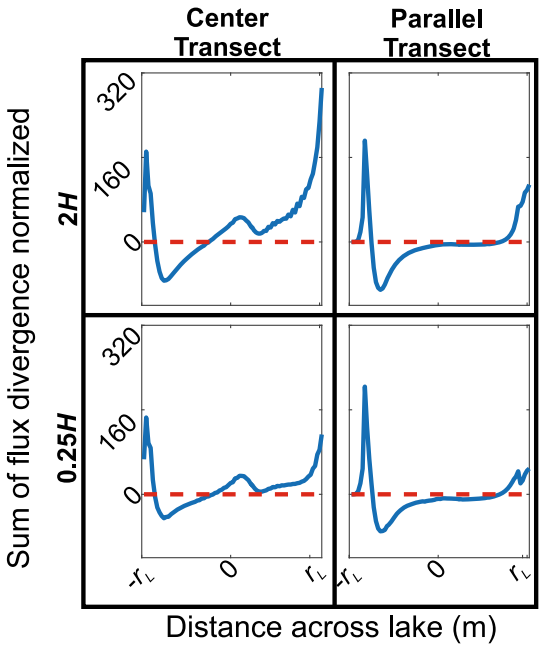

Fig. 9 *Simulation 2*. Sum of flux divergence for a transect through the centre-line of the lake (*left column*) and a parallel transect 100 m off-centre (*right column*) for the high tower (*top row*) and the low tower (*bottom row*). The scalars originating from the lake are shown, but the patterns are representative of the forest for all scalars considered together

A symmetric pattern of flux divergence developed across the lake area parallel to the prevailing wind direction, which features a wedge-shaped area at the focal point in the lake's centre, and expands towards the downwind edge of the lake where total flux divergence increases relative to the surrounding area (Fig. 8). This wedge is created by the upwards advection observed in Fig. 3, and as the flux becomes large near the top of the canopy, this induces a significant flux divergence.

The areas near the edges of the lake are characterized by high divergence for both the low- and high-tower scenarios (Fig. 9). However, just downwind of the centre of the lake (around location $T4$), the total flux divergence dips to near-zero values and remains virtually constant until close to the downwind transition. As this pattern is evident in all scalar-height combinations, this further supports the possibility that location $T4$ may be a promising, if not optimal, location for eddy-covariance measurements. Unexpectedly, the total flux divergence of the off-centre transect remains fairly constant and near-zero for a substantial distance across the lake (Fig. 9). However, the off-centre location is dependent on the wind direction and, with shifting wind directions, is not a fixed location. Furthermore, as the results for an off-centre transect would be more difficult to interpret for more realistic lake geometries (i.e. non-circular), more comprehensive simulations are needed to generalize this finding. As many lakes are oblong (e.g. Vesala et al. 2006) or non-circular, additional considerations of more complex lake geometry merit future investigation for the determination of the optimal tower location.

4 Conclusions

We performed a numerical study of a small circular lake surrounded by forest to examine potential biases to eddy-covariance measurements. Our RAFLES-based model analyses of scalar dispersion demonstrated that such a lake poses significant challenges for eddy-

covariance measurements, with results showing that lake-scale and canopy-scale secondary circulations drive complex persistent patterns of horizontal and vertical advection of scalars such as CO_2, emitted by the lake and forest. These phenomena will generate biases in eddy-covariance observations for which the current, standard analytical footprint models are unable to take into account.

One effect of secondary circulations is the formation of persistent vertical jets and downdrafts near the forest-lake transitions, which contribute to fluxes, but are neglected by standard processing procedures of eddy-covariance measurements, which assume a zero vertical velocity component. The use of the standard three-dimensional axis rotation during the 30-min averaged simulations presented here would result, for many 30-min periods, in a highly biased flux measurement due to an erroneous rotation of the coordinate plane to an unrealistically steep angle (Fig. 3). We recommend that three-dimensional axis rotations be excluded in flux-processing procedures for these ecosystems. Rather, researchers can minimize the need for this correction by careful, independent levelling of the sonic anemometer, which is frequently difficult to achieve, particularly due to tower sway induced by wind and wave action. However, advances in electronic gyroscopes and accelerometers should help improve the accuracy of wind-independent coordinate levelling.

While the vertical flux divergence can be used as an indicator of the influence of horizontal advection on total flux calculations, it remains impossible to differentiate the contributions of lake versus forest fluxes when measuring at a single point in real-world measurement systems. We confirm that effects from advection are minimized by using a low ratio of measurement height to distance to the upwind shore in agreement with Higgins et al. (2013). However, in reality, the distance to the upwind edge of a lake may vary with shifting wind directions, which will complicate interpretation. As such, actual flux towers may require additional filtering procedures when treating lake flux data. Practical considerations assessed here include the placement of the tower at an adequate distance downwind from the edge in the primary wind direction, and the calculation of the height to distance from lake edge ratio. These values should then be compared with the threshold set by Higgins et al. (2013), $z_1/D_T < 0.02$, for each averaging interval. Observations from times with prevailing wind directions that fail this criterion should be flagged as potentially biased and eliminated from the overall flux analysis. The lake-radius to canopy-height ratio could be altered to generalize the results found here, where we simulated a lake with a radius of ten times the canopy height. For example, wider lakes will have a broader range of valid measurement locations. While smaller lakes possess fewer valid locations, we find that so long as the Higgins et al. (2013) ratio is followed, flux measurements are minimally affected by vertical advection.

While our study is limited to a specific lake/forest geometry with a homogenous canopy, recent literature suggests that these results have broader implications. Forest inhomogeneities add layers of complexity to the simulation not considered here, which, according to other studies, introduce so-called enhanced gust zones consisting of non-uniform airflow patterns over the canopy (Bohrer et al. 2009; Dupont and Brunet 2008a). Enhanced gust zones are similar to the rotor effects demonstrated here in that they cause areas of high advection resulting from structural heterogeneity. Variations in the canopy structure have also been shown to enhance flow penetration into the canopy itself, which may affectthe rotor effect immediately downwind of the lake/forest transition (Boudreault et al. 2016) and, correspondingly, affect the true flow of trace gases to the lake surface from the upwind canopy. However, due to the relatively low levels of fluxes associated with the lake surface compared with those advected, forest canopy effects are unlikely to significantly alter the results shown here. Furthermore, the heterogeneity of the lake/forest transition is far more drastic and has much stronger effects than the structure of the canopy and so these transitions will dominate advective behaviour

near the transition and over the lake surface. Similarly, the heterogeneous treatment of the lake surface to account for near-shore plant communities or roughness as a function of the wind speed would alter the effects shown here. However, roughness heterogeneity is also very unlikely to have significantly altered the advective patterns due to the order-of-magnitude difference between those heterogeneities and the lake/forest transition.

Additional simulations could establish the effect of varying the size and shape of the lake, but, again, these changes are unlikely to significantly alter the conclusions reached here. Dupont and Brunet (2008b) showed the effects of a sharp linear transition to a forest having similar updrafts to those shown here. Damschen et al. (2014) performed similar simulations with square clearings and demonstrated large-scale circulations such as those shown here. Recently, the analysis of Eder et al. (2015), using eddy-covariance measurements in conjunction with LES, demonstrated comparable effects of secondary circulations in a patch of forest surround by desert. The synthesis of these results demonstrates that, with further evaluation, the recommendations generated by our scenario of a forest surrounding a lake are broadly applicable to other heterogeneous land surfaces with sharp heat-flux and roughness discontinuities.

Acknowledgements The study was funded by the NASA Earth and Space Science Graduate Training Fellowship #NNX11AL45H to WTK, and National Science Foundation (NSF) Hydrological Science award #1521238. Flux observations at the UMBS tower are supported by U.S. Department of Energy's Office of Science, Ameriflux Management project under Flux Core Site agreement No. 7096915 through the Lawrence Berkeley National Laboratory. The LES-based footprint approach was developed with support from the NSF CBET award #1508994. The simulation ran at the Ohio Supercomputer Center, under computation allocation grant #PAS0409-4. THM was funded in part by NSF Doctoral Dissertation Improvement Grant #DEB-1601224 and the Department of Energy Office of Science Graduate Research Program, 2015. ARD acknowledges support from the NSF North Temperate Lakes LTER cooperative agreement (DEB-1440297).

References

Anderson DE, Striegl RG, Stannard DI, Michmerhuizen CM, McConnaughey TA, LaBaugh JW (1999) Estimating lake-atmosphere CO_2 exchange. Limnol Oceanogr 44(4):988–1001

Aubinet M, Feigenwinter C, Heinesch B, Bernhofer C, Canepa E, Lindroth A, Montagnani L, Rebmann C, Sedlak P, Van Gorsel E (2010) Direct advection measurements do not help to solve the night-time CO_2 closure problem: evidence from three different forests. Agric For Meteorol 150(5):655–664

Aubinet M, Vesala T, Papale D (2012) Eddy covariance: a practical guide to measurement and data analysis. Springer Science & Business Media, Berlin, 438 pp

Barr AG, Richardson AD, Hollinger DY, Papale D, Arain MA, Black TA, Bohrer G, Dragoni D, Fischer ML, Gu L, Law BE, Margolis HA, McCaughey JH, Munger JW, Oechel W, Schaeffer K (2013) Use of change-point detection for friction-velocity threshold evaluation in eddy-covariance studies. Agric For Meteorol 171:31–45

Bastviken D, Tranvik LJ, Downing JA, Crill PM, Enrich-Prast A (2011) Freshwater methane emissions offset the continental carbon sink. Science 331:50–50

Belcher SE, Harman IN, Finnigan JJ (2012) The wind in the willows: flows in forest canopies in complex terrain. Annu Rev Fluid Mech 44:479–504

Bohrer G (2007) Large eddy simulations of forest canopies for determination of biological dispersal by wind. PhD Thesis, Duke University, Durham, NC, p 150

Bohrer G, Katul GG, Nathan R, Walko RL, Avissar R (2008) Effects of canopy heterogeneity, seed abscission, and inertia on wind-driven dispersal kernels of tree seeds. J Ecol 96:569–580

Bohrer G, Katul GG, Walko RL, Avissar R (2009) Exploring the effects of microscale structural heterogeneity of forest canopies using large-eddy simulations. Boundary-Layer Meteorol 132:351–382

Boudreault, LÉ, Dupont S, Bechmann A, Dellwik E (2016) How forest inhomogeneities affect the edge flow. Boundary-Layer Meteorol 162(3):375–400

Cassiani M, Katul GG, Albertson JD (2008) The effects of canopy leaf area index on airflow across forest edges: large eddy simulation and analytical results. Boundary-Layer Meteorol 126:433–460

Chatziefstratiou EK, Velissariou V, Bohrer G (2014) Resolving the effects of aperture and volume restriction of the flow by semi-porous barriers using large-eddy simulations. Boundary-Layer Meteorol 152(3):329–348

Cole JJ, Prairie YT, Caraco NF, McDowell WH, Tranvik LJ, Striegl RG, Duarte CM, Kortelainen P, Downing JA, Middelburg JJ, Melack J (2007) Plumbing the global carbon cycle: integrating inland waters into the terrestrial carbon budget. Ecosystems 10(1):172–185. doi:10.1007/s10021-006-9013-8

Damschen EI, Baker DV, Bohrer G, Nathan R, Orrock JL, Turner JR, Tewksbury JJ (2014) How fragmentation and corridors affect wind dynamics and seed dispersal in open habitats. Proc Natl Acad Sci 111(9):3484–3489

Deardorff JW (1980) Stratocumulus-capped mixed layers derived from a 3-dimensional model. Boundary-Layer Meteorol 18(4):495–527

Detto M, Katul GG, Siqueira M, Juang J-H, Stoy PC (2008) The structure of turbulence near a tall forest edge: the backward facing step flow analogy revisited. Ecol Appl 18(6):1420–1435

Detto M, Montaldo N, Albertson JD, Mancini M, Katul G (2006) Soil moisture and vegetation controls on evapotranspiration in a heterogeneous Mediterranean ecosystem on Sardinia, Italy. Water Resour Res 42(8):W08419

Downing J, Prairie Y, Cole J, Duarte C, Tranvik L, Striegl R, McDowell W, Kortelainen P, Caraco N, Melack J (2006) The global abundance and size distribution of lakes, ponds, and impoundments. Limnol Oceanogr 51(5):2388–2397

Duchemin E, Lucotte M, Canuel R (1999) Comparison of static chamber and thin boundary layer equation methods for measuring greenhouse gas emissions from large water bodies. Environ Sci Technol 33(2):350–357

Dupont S, Brunet Y (2008a) Edge flow and canopy structure: a large-eddy simulation study. Boundary-Layer Meteorol 126(1):51–71

Dupont S, Brunet Y (2008b) Influence of foliar density profile on canopy flow: a large-eddy simulation study. Agric For Meteorol 148(6–7):976–990

Dupont S, Bonnefond J-M, Irvine MR, Lamaud E, Brunet Y (2011) Long-distance edge effects in a pine forest with a deep and sparse trunk space: in situ and numerical experiments. Agric For Meteorol 151(3):328–344

Eder F, De Roo F, Rotenberg E, Yakir D, Schmid HP, Mauder M (2015) Secondary circulations at a solitary forest surrounded by semi-arid shrubland and their impact on eddy-covariance measurements. Agric For Meteorol 211:115–127

Eugster W, DelSontro T, Sobek S (2011) Eddy covariance flux measurements confirm extreme CH (4) emissions from a Swiss hydropower reservoir and resolve their short-term variability. Biogeosciences 8(9):2815–2831

Eugster W, Kling G, Jonas T, McFadden JP, Wüest A, MacIntyre S, Chapin FS (2003) CO2 exchange between air and water in an Arctic Alaskan and midlatitude Swiss lake: importance of convective mixing. J Geophys Res Atmos 108:4362

Feng M, Sexton JO, Channan S, Townshend JR (2016) A global, high-resolution (30-m) inland water body dataset for 2000: first results of a topographic-spectral classification algorithm. Int J Digit Earth 9(2):113–133

Finnigan JJ, Clement R, Malhi Y, Leuning R, Cleugh HA (2003) A re-evaluation of long-term flux measurement techniques—part I: averaging and coordinate rotation. Boundary-Layer Meteorol 107(1):1–48

Forster P, Ramaswamy V, Artaxo P, Berntsen T, Betts R, Fahey DW, Haywood J, Lean J, Lowe DC, Myhre G (2007) Changes in atmospheric constituents and in radiative forcing. Chapter 2. Climate change 2007, The physical science basis

Froelich NJ, Schmid HP (2006) Flow divergence and density flows above and below a deciduous forest—part II. Below-canopy thermotopographic flows. Agric For Meteorol 138(1–4):29–43

Froelich NJ, Schmid HP, Grimmond CSB, Su HB, Oliphant AJ (2005) Flow divergence and density flows above and below a deciduous forest. Part I. Non-zero mean vertical wind above canopy. Agric For Meteorol 133(1–4):140–152

Gough C, Bohrer G, Curtis P (2016) AmeriFlux US-UMB University of Michigan Biological Station. doi:10.17190/AMF/1246107

Gough CM, Flower CE, Vogel CS, Dragoni D, Curtis PS (2009) Whole-ecosystem labile carbon production in a north temperate deciduous forest. Agric For Meteorol 149(9):1531–1540

Gough CM, Hardiman BS, Nave LE, Bohrer G, Maurer KD, Vogel CS, Nadelhoffer KJ, Curtis PS (2013) Sustained carbon uptake and storage following moderate disturbance in a Great Lakes forest. Ecol Appl 23(5):1202–1215

Hardiman BS, Bohrer G, Gough CM, Vogel CS, Curtis PS (2011) The role of canopy structural complexity in wood net primary production of a maturing northern deciduous forest. Ecology 92(9):1818–1827

Higgins CW, Pardyjak E, Froidevaux M, Simeonov V, Parlange MB (2013) Measured and estimated water vapor advection in the atmospheric surface layer. J Hydrometeorol 14(6):1966–1972

Hsieh CI, Katul G, Chi T (2000) An approximate analytical model for footprint estimation of scaler fluxes in thermally stratified atmospheric flows. Adv Water Resour 23(7):765–772

Huotari J, Ojala A, Peltomaa E, Nordbo A, Launiainen S, Pumpanen J, Rasilo T, Hari P, Vesala T (2011) Long-term direct CO_2 flux measurements over a boreal lake: five years of eddy covariance data. Geophys Res Lett 38. doi:10.1029/2011gl048753

Knox SH, Sturtevant C, Matthes JH, Koteen L, Verfaillie J, Baldocchi D (2015) Agricultural peatland restoration: effects of land-use change on greenhouse gas (CO_2 and CH_4) fluxes in the Sacramento–San Joaquin Delta. Global Change Biol 21(2):750–765

Lee X, Finnigan JJ, Paw UKT (2004) Coordinate systems and flux bias error. In: Lee X, Massman W, Law B (eds) Handbook of micrometeorology, a guide for surface flux measurement and analysis. Kluwer Academic Publishers, Dordrecht, pp 33–66

MacIntyre S, Eugster W, Kling GW (2002) The critical importance of buoyancy flux for gas flux across the air-water interface. In: Donelan MA, Drennan WM, Saltzman ES, Wanninkhof R (eds) Gas transfer at water surfaces. American Geophysical Union, Washington, pp 135–139

Mammarella I, Nordbo A, Rannik Ü, Haapanala S, Levula J, Laakso H, Ojala A, Peltola O, Pumpanen J, Heiskanen J (2015) Carbon dioxide and energy fluxes over a small boreal lake in Southern Finland. J Geophys Res Biogeosci 120(7):1296–1314

Matheny AM, Bohrer G, Vogel CS, Morin TH, He L, Frasson RPdM, Mirfenderesgi G, Schäfer KV, Gough CM, Ivanov VY (2014) Species-specific transpiration responses to intermediate disturbance in a northern hardwood forest. J Geophys Res Biogeosci 119(12):2292–2311

Maurer K, Bohrer G, Kenny W, Ivanov V (2015) Large-eddy simulations of surface roughness parameter sensitivity to canopy-structure characteristics. Biogeosciences 12(8):2533–2548

Morin TH, Bohrer G, Naor-Azrieli L, Mesi S, Mitsch WJ, Schäfer KVR (2014) The seasonal and diurnal dynamics of methane flux at a created urban wetland. Ecol Eng 72:74–83

Morin TH, Rey-Sánchez AC, Vogel CS, Matheny AM, Kenny WT, Bohrer G (2017a) Carbon dioxide emissions from an oligotrophic temperate lake: an eddy covariance approach. Ecol Eng. doi:10.1016/j.ecoleng.2017.05.005 (In press)

Morin TH, Bohrer G, Stefanik KC, Rey-Sanchez AC, Matheny AM, Mitsch WJ (2017b) Combining eddy-covariance and chamber measurements to determine the methane budget from a small, heterogeneous urban floodplain wetland park. Agric For Meteorol 237:160–170. doi:10.1016/j.agrformet.2017.01.022

Novick K, Brantley S, Miniat CF, Walker J, Vose J (2014) Inferring the contribution of advection to total ecosystem scalar fluxes over a tall forest in complex terrain. Agric For Meteorol 185:1–13

Podgrajsek E, Sahlée E, Rutgersson A (2015) Diel cycle of lake-air CO_2 flux from a shallow lake and the impact of waterside convection on the transfer velocity. J Geophys Res Biogeosci 120(1):29–38

Reichstein M, Falge E, Baldocchi D, Papale D, Aubinet M, Berbigier P, Bernhofer C, Buchmann N, Gilmanov T, Granier A, Grunwald T, Havrankova K, Ilvesniemi H, Janous D, Knohl A, Laurila T, Lohila A, Loustau D, Matteucci G, Meyers T, Miglietta F, Ourcival JM, Pumpanen J, Rambal S, Rotenberg E, Sanz M, Tenhunen J, Seufert G, Vaccari F, Vesala T, Yakir D, Valentini R (2005) On the separation of net ecosystem exchange into assimilation and ecosystem respiration: review and improved algorithm. Global Change Biol 11(9):1424–1439

Schubert CJ, Diem T, Eugster W (2012) Methane emissions from a small wind shielded lake determined by eddy covariance, flux chambers, anchored funnels, and boundary model calculations: a comparison. Environ Sci Technol 46(8):4515–4522

Sellers P, Hesslein RH, Kelly CAK (1995) Continuous measurement of CO_2 for estimation of air-water fluxes in lakes: an in situ technique. Limnol Oceanogr 40(3):575–581

Stoll R, Porté-Agel F (2009) Surface heterogeneity effects on regional-scale fluxes in stable boundary layers: surface temperature transitions. J Atmos Sci 66(2):412–431

Striegl RG, Kortelainen P, Chanton JP, Wickland KP, Bugna GC, Rantakari M (2001) Carbon dioxide partial pressure and 13C content of north temperate and boreal lakes at spring ice melt. Limnol Oceanogr 46(4):941–945

Su H-B, Schmid H, Grimmond C, Vogel C, Curtis P (2008) An assessment of observed vertical flux divergence in long-term eddy-covariance measurements over two Midwestern forest ecosystems. Agric For Meteorol 148(2):186–205

Tranvik LJ, Downing JA, Cotner JB, Loiselle SA, Striegl RG, Ballatore TJ, Dillon P, Finlay K, Fortino K, Knoll LB (2009) Lakes and reservoirs as regulators of carbon cycling and climate. Limnol Oceanogr 54:2298–2314

Van Gorsel E, Delpierre N, Leuning R, Black A, Munger JW, Wofsy S, Aubinet M, Feigenwinter C, Beringer J, Bonal D (2009) Estimating nocturnal ecosystem respiration from the vertical turbulent flux and change in storage of CO_2. Agric For Meteorol 149(11):1919–1930

Vesala T, Eugster W, Ojala A (2012) Eddy covariance measurements over lakes. In: Aubinet M, Vesala T, Papale D (eds) Eddy covariance, vol 111. Springer, New York, pp D11101

Vesala T, Huotari J, Rannik Ü, Suni T, Smolander S, Sogachev A, Launiainen S, Ojala A (2006) Eddy covariance measurements of carbon exchange and latent and sensible heat fluxes over a boreal lake for a full open-water period. J Geophys Res Atmos 111(D11). doi:10.1029/2005jd006365

Walko RL, Tremback CJ (2001) RAMS technical description